Special Issue Article

Advances in Mechanical Engineering

Advances in Mechanical Engineering
2017, Vol. 9(11) 1–11

DOI: 10.1177/1687814017737449
journals.sagepub.com/home/ade
SAGE

A reliability-based robust design for structural components with a variable cross section under limited probabilistic information

Tianxiao Zhang and David He

Abstract

In engineering design, structural components with variable cross sections are extensively employed due to their excellent mechanical properties. From a strength and stiffness perspective, structural components with a uniform cross section are not always ideal. Therefore, to effectively utilize material, variable cross section structural components with excellent properties such as high strength and stiffness are employed in many practical engineering applications. As a multi-dimensional function is required to describe the state of a variable cross section structural component, determining the locations of its dangerous cross sections is very difficult. As a result, the development of a reliability-based design for a variable cross section structural component is a complex process. Therefore, strict theoretical derivations and reasonable quantitative research are required to understand the variation pattern of the reliability of the variable cross section structural component with the coordinates to determine the locations of its dangerous cross sections. This article presents a reliability sensitivity analysis with limited probabilistic information and a reliability-based robust design variable cross section structural component. Mathematical models for reliability sensitivity analysis and reliability-based robust design of variable cross section structural components with incomplete probabilistic information are established. Reliability sensitivity analysis and reliability-based robust design methods for variable cross section structural components with non-normally distributed parameters are proposed. The article provides the changing condition of the reliability with respect to the variable cross section, describes the change rule of reliability with respect to design parameters, and provides the multi-objective optimal design model based on reliability sensitivity. The reliability index obtained using the presented method is insensitive and therefore robust. Using a numerical example, the variation curves of the reliability index and reliability of a variable cross section structural component with coordinates of variable cross section are obtained. A reliability-based robust optimal design approach for variable cross section structural components for given design reliability index conditions is provided.

Keywords

Structural component with a variable cross section, incomplete probabilistic information, reliability, reliability sensitivity analysis, reliability-based robust design

Date received: 20 June 2017; accepted: 26 September 2017

Handling Editor: Shun-Peng Zhu

Introduction

In engineering design, structural components with a variable cross section (VCS structural components) are extensively employed due to their excellent mechanical

Department of Mechanical & Industrial Engineering, University of Illinois at Chicago, Chicago, IL, USA

Corresponding author:
David He, Department of Mechanical & Industrial Engineering, University of Illinois at Chicago, Chicago, IL 60607, USA.
Email: davidhe@uic.edu

Figure 1. VCS steel beam.

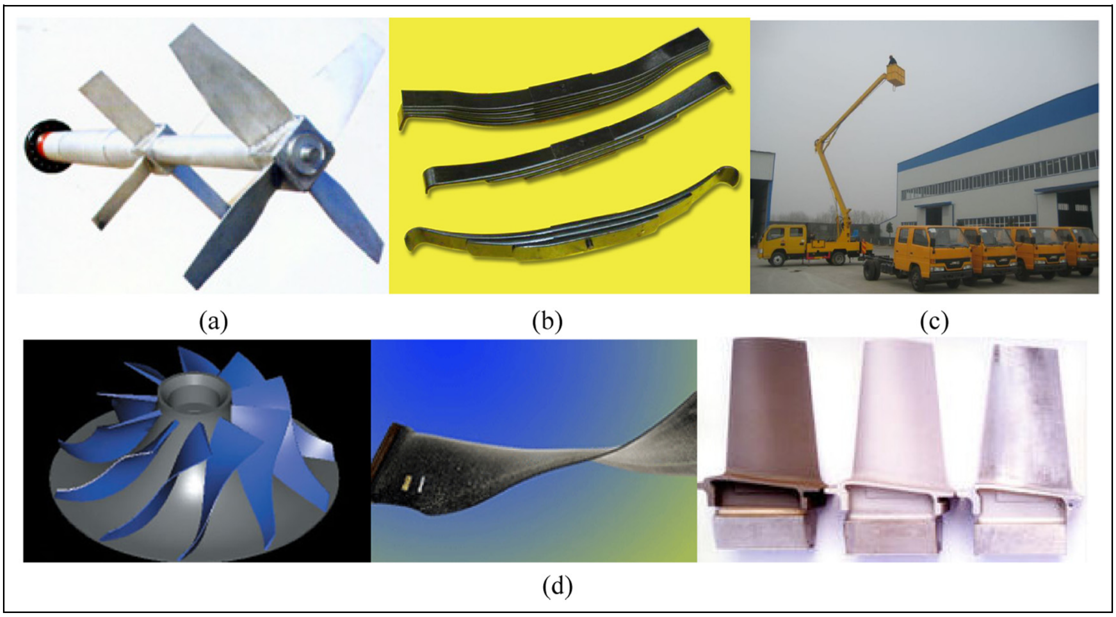

Figure 2. VCS parts: (a) VCS stirring blade, (b) VCS leaf spring, (c) VCS composite box beam, and (d) VCS blade.

properties, for example, VCS beams, which are employed in large numbers in construction engineering applications (Figure 1), and VCS parts, which are extensively employed in mechanical equipment (Figure 2). VCS structural components are ubiquitous in everyday life and practical engineering applications. Lightweight, low-cost, and high-performance VCS structural components are employed in large numbers in fields such as aerospace, mechanical machinery, and civil engineering. An ideal structural component should have large cross sections at locations where large bending moments and deformation occur and small cross sections at locations where small bending moments and deformation occur. Consequently, an ideal structural component has a cross section that varies in size along with its length and excellent properties (e.g. high strength and stiffness). Thus, the use of VCS structural components can facilitate material saving, weight and cost reduction, and performance enhancement. Therefore, investigating reliability and reliability sensitivity problems concerning VCS structural components has application and academic values.

Reliability, which is an important structure quality index, is garnering increasing attention from engineering industries. Of the three stages (design, production, and application), modern production practice demonstrates that design determines the reliability level of a structural component (i.e. inherent reliability of a structural component), and production and application ensure the realization of the reliability index β of the structural component. Numerous excellent results have been achieved using reliability analysis and reliability-based design methods based on probability and statistics.[1–11]

As different factors affect the reliability of a structural component to varying degrees, the reliability sensitivity of the structural component should be sufficiently analyzed. Using a reliability sensitivity analysis, the impact of the variations in the design parameters on the reliability of a structural component can be evaluated, which reveals the level of impact of each design parameter on the reliability of the structural component, that is, sensitivity.[12–15]

For a structural reliability-based robust design, reliability sensitivity is included in an optimal design model based on a reliability-based design, an optimal design, a sensitivity-based design, and a robust design, and the reliability-based robust design is converted to a multi-objective optimal design that satisfies the reliability requirements. As a low-cost, high-reliability design concept and method,[16–22] Lagaros et al.[23] implemented a combined reliability-based robust design optimization (RRDO) formulation. Yadav et al.[24] established new and effective techniques and tools to ensure a robust and reliable product design. Wang et al.[25] proposed a unified framework for integrating reliability-based design and robust design. Wang et al.[26] attempts to integrate reliability, maintenance, and warranty during reliability-based design. Martowicz and Uhl[27] discussed the applicability of a reliability- and performance-based multi-criteria robust design optimization technique for micro-electromechanical systems. Yu et al.[28] proposed in their work a reliability-based robust design optimization framework dedicated to the tuned mass damper in passive vibration control. Paiva et al.[29] outlined an architecture for simultaneous analysis and calculation of robustness and reliability in aircraft wing design optimization. Wang et al.[30] presented a new approach to efficiently carry out dynamic reliability analysis for RRDO. Qui et al.[31] proposed a reliability-based robust design approach on the basis of axiomatic theory, aiming at actualizing a reliability-based robust design framework for mechanism motion.

Many researches based on VCS have been reported. Boiangiu et al.[32] provided differential equations for free bending vibrations of straight beams with VCS using Bessel's functions. Kang et al.[33] investigated the methodology to enhance hydroformability of non-axisymmetric thin-wall tubular component with VCS. Li et al.[34] provided a transfer matrix method used to predict the transmission loss of apertures assuming that the cross-sectional dimensions are small compared to an acoustic wavelength. Jun et al.[35] studied a flexible extrusion process which involves extruding the materials via one fixed and one movable die.

Currently, most reliability analysis techniques for VCS structural components in mechanical equipment are developed based on accumulated experience or experiments. The failure mechanisms of VCS structural components have not been completely revealed, and reliability-based design models for VCS structural components have not been clearly established; consequently, the available reliability-based design models lack ideal accuracy and precision. Currently, research on reliability-based design of VCS structural components is in the early stage, and no research has been conducted on reliability sensitivity analysis and reliability-based robust design of VCS structural components.

In this study, based on preliminary theoretical research on structural reliability, a reliability sensitivity analysis is performed on VCS structural components, and a reliability-based robust design is developed with incomplete probabilistic information using theoretical methods such as structural reliability-based design, reliability sensitivity analysis, and reliability-based robust design. In addition, a reliability sensitivity analysis is performed on VCS structural components with non-normally distributed parameters, and a reliability-based robust design is developed for these structural components using modern mathematical and mechanical theories and methods, such as probability and statistics theory, stochastic perturbation technique, higher-order moment method, reliability-based design technique, sensitivity theory, and robust design method. Engineering reliability sensitivity analysis and reliability-based robust design methods for VCS structural components using limited probabilistic information are proposed. The problem of whether the reliability of VCS structural components is sensitive to the design parameters is discussed. For the condition in which the probabilistic characteristics of the basic random variables are known, information that relates to the reliability sensitivity analysis and reliability-based robust design of a VCS structural component can be rapidly and accurately obtained.

Reliability analysis method

One goal of structural reliability analysis is to determine the reliability of the system

$$R = \int_{g_z(\boldsymbol{X})>0} f_{\boldsymbol{X}}(\boldsymbol{X})\mathrm{d}\boldsymbol{X} \tag{1}$$

where $f_{\boldsymbol{X}}(\boldsymbol{X})$ is the joint probability density function of the basic random parameter vectors ($\boldsymbol{X} = (X_1 X_2 \cdots X_n)^{\mathrm{T}}$); z is the coordinate variable of the VCS structural component; and $g_z(\boldsymbol{X})$ is the state function of the VCS structural component that varies with z, which describes the safety and failure states, that is

$$g_z(\boldsymbol{X}) = r - S_z(\boldsymbol{X}) \tag{2}$$

where r represents the strength of the material; S_z represents the stress of the VCS structural component that varies with z; and $\boldsymbol{X}$ represents the random variable vectors. $g_z(\boldsymbol{X})$ can indicate two states of the structural component, that is

$$\left.\begin{array}{ll} g_z(X) \leq 0 & \text{failurestate} \\ g_z(X) > 0 & \text{safestate} \end{array}\right\} \tag{3}$$

The first four moments of $g_z(\boldsymbol{X})$ can be expressed as follows[36]

$$\mu_{g_z} = \mathrm{E}[g_z(\boldsymbol{X})] = \bar{g}_z(\boldsymbol{X}) \approx g_z\left(\boldsymbol{X}\right) = g_z[\boldsymbol{\mu}(\boldsymbol{X})] \tag{4}$$

$$\sigma_{g_z}^2 = \mathrm{Var}[g_z(\boldsymbol{X})] = \frac{\partial g_z(\boldsymbol{X})}{\partial \boldsymbol{X}^{\mathrm{T}}} \mathrm{C}_2(\boldsymbol{X}) \frac{\partial g_z(\boldsymbol{X})}{\partial \boldsymbol{X}} \tag{5}$$

$$\theta_{g_z} = \mathrm{E}\left[\left(g_z(\boldsymbol{X}) - \mu_{g_z}\right)^3\right] = \frac{\partial g_z(X)}{\partial \boldsymbol{X}^{\mathrm{T}}} \mathrm{C}_3(\boldsymbol{X}) \frac{\partial g_z(\boldsymbol{X})}{\partial \boldsymbol{X}} \otimes \frac{\partial g_z(\boldsymbol{X})}{\partial \boldsymbol{X}} \tag{6}$$

$$\eta_{g_z} = \mathrm{E}\left[\left(g_z(\boldsymbol{X}) - \mu_{g_z}\right)^4\right] = \frac{\partial g_z(\boldsymbol{X})}{\partial \boldsymbol{X}^{\mathrm{T}}} \otimes \frac{\partial g_z(\boldsymbol{X})}{\partial \boldsymbol{X}^{\mathrm{T}}} \mathrm{C}_4(\boldsymbol{X}) \frac{\partial g_z(\boldsymbol{X})}{\partial \boldsymbol{X}} \otimes \frac{\partial g_z(\boldsymbol{X})}{\partial \boldsymbol{X}} \tag{7}$$

where $\otimes$ represents the Kronecker product, and $\boldsymbol{\mu}(\boldsymbol{X})$, $\mathbf{C}_2(\boldsymbol{X})$, $\mathbf{C}_3(\boldsymbol{X})$, and $\mathbf{C}_4(\boldsymbol{X})$ represent the mean, covariance, third-moment, and fourth-moment matrices, respectively, of the random variables of the structural component ($\boldsymbol{X}$).

When the first two moments of the basic random parameters of the structural component ($\boldsymbol{X} = (X_1X_2 \cdots X_n)^{\mathrm{T}}$), that is, the mean vector ($\mathrm{E}(\boldsymbol{X})$) and $\mathbf{C}_2(\boldsymbol{X})$ are known, β can be expressed using the second-moment method (β_{SM}) as follows

$$\beta_{\mathrm{SM}} = \frac{\mu_{g_z}}{\sigma_{g_z}} = \frac{\mathrm{E}[g_z(\boldsymbol{X})]}{\sqrt{\mathrm{Var}[g_z(\boldsymbol{X})]}} \tag{8}$$

When $\boldsymbol{X} = (X_1X_2 \cdots X_n)^{\mathrm{T}}$ each completely follow a normal distribution, a first-order approximate estimate of the reliability of the structural component can be obtained using the second-moment method (R_{SM})

$$R_{\mathrm{SM}} = \Phi(\beta_{\mathrm{SM}}) \tag{9}$$

where $\Phi(\cdot)$ represents a standard normal distribution function.

When $\boldsymbol{X} = (X_1X_2 \cdots X_n)^{\mathrm{T}}$ each follow a non-normal distribution, if approximate estimates of the first four moments of $\boldsymbol{X} = (X_1X_2 \cdots X_n)^{\mathrm{T}}$ (i.e. $\mathrm{E}(\boldsymbol{X})$, $\mathbf{C}_2(\boldsymbol{X})$, $\mathbf{C}_3(\boldsymbol{X})$, and $\mathbf{C}_4(\boldsymbol{X})$) are known, β can be defined using the higher-moment method (β_{FM}) as follows[37]

$$\beta_{\mathrm{FM}} = \frac{6\left(3\alpha_{4g_z} + 2\right)\beta_{\mathrm{SM}} + 11\alpha_{3g_z}\left(\beta_{\mathrm{SM}}^2 - 1\right)}{\sqrt{36\left(3\alpha_{4g_z} + 2\right)^2 - 55\alpha_{3g_z}^2\left(5\alpha_{4g_z} + 7\right)}} \tag{10a}$$

$$\beta_{\mathrm{FM}} = \frac{6\mu_{g_z}\left(3\eta_{g_z} + 2\sigma_{g_z}^4\right) + 11\theta_{g_z}\left(\mu_{g_z}^2 - \sigma_{g_z}^2\right)}{\sqrt{36\sigma_{g_z}^2\left(3\eta_{g_z} + 2\sigma_{g_z}^4\right)^2 - 55{\theta_{g_z}}^2\left(5\eta_{g_z} + 7\sigma_{g_z}^4\right)}} \tag{10b}$$

where $\alpha_{3g_z} = \theta_{g_z}/\sigma_{g_z}^3$ and $\alpha_{4g_z} = \eta_{g_z}/\sigma_{g_z}^4$ are the coefficient of skewness and the coefficient of kurtosis of $g(\boldsymbol{X})$, respectively.

When the distribution of $\boldsymbol{X} = (X_1X_2 \cdots X_n)^{\mathrm{T}}$ cannot be determined, the β_{FM} of the structural component can be calculated using the higher-moment method based on which an approximate estimate of the reliability (R_{FM}) can be determined, that is

$$R_{\mathrm{FM}} = \Phi(\beta_{\mathrm{FM}}) \tag{11}$$

Thus, the reliability of the structural component is obtained; in addition, a reliability analysis can be performed on the structural component and a reliability-based design can be developed.

Reliability sensitivity analysis

When the first four moments of $\boldsymbol{X} = (X_1X_2 \cdots X_n)^{\mathrm{T}}$ are known, although the distribution of $\boldsymbol{X}$ cannot be determined, a reliability analysis and reliability-based design for the structural component can be performed based on the high-moment method for reliability-based design. Based on β_{FM} and R_{FM} (defined by the high-moment method for reliability analysis and reliability-based design), the reliability sensitivity to the mean vector $\boldsymbol{\mu}_{\boldsymbol{X}} = \mathrm{E}(\boldsymbol{X})$ and standard deviation vector $\boldsymbol{\sigma}_{\boldsymbol{X}}$ of $\boldsymbol{X} = (X_1X_2 \cdots X_n)^{\mathrm{T}}$, respectively, are obtained by the following derivations

$$\frac{\partial R_{\mathrm{FM}}}{\partial \boldsymbol{\mu}_X^{\mathrm{T}}} = \frac{\partial R_{\mathrm{FM}}}{\partial \beta_{\mathrm{FM}}} \left[\frac{\partial \beta_{\mathrm{FM}}}{\partial \mu_{g_z}} \frac{\partial \mu_{g_z}}{\partial \boldsymbol{\mu}_X^{\mathrm{T}}} + \frac{\partial \beta_{\mathrm{FM}}}{\partial \sigma_{g_z}} \frac{\partial \sigma_{g_z}}{\partial \boldsymbol{\mu}_X^{\mathrm{T}}} + \frac{\partial \beta_{\mathrm{FM}}}{\partial \theta_{g_z}} \frac{\partial \theta_{g_z}}{\partial \boldsymbol{\mu}_X^{\mathrm{T}}} + \frac{\partial \beta_{\mathrm{FM}}}{\partial \eta_{g_z}} \frac{\partial \eta_{g_z}}{\partial \boldsymbol{\mu}_X^{\mathrm{T}}}\right] \tag{12}$$

$$\frac{\partial R_{\mathrm{FM}}}{\partial \boldsymbol{\sigma}_X^{\mathrm{T}}} = \frac{\partial R_{\mathrm{FM}}}{\partial \beta_{\mathrm{FM}}} \left[\frac{\partial \beta_{\mathrm{FM}}}{\partial \mu_{g_z}} \frac{\partial \mu_{g_z}}{\partial \boldsymbol{\sigma}_X^{\mathrm{T}}} + \frac{\partial \beta_{\mathrm{FM}}}{\partial \sigma_{g_z}} \frac{\partial \sigma_{g_z}}{\partial \boldsymbol{\sigma}_X^{\mathrm{T}}} + \frac{\partial \beta_{\mathrm{FM}}}{\partial \theta_{g_z}} \frac{\partial \theta_{g_z}}{\partial \boldsymbol{\sigma}_X^{\mathrm{T}}} + \frac{\partial \beta_{\mathrm{FM}}}{\partial \eta_{g_z}} \frac{\partial \eta_{g_z}}{\partial \boldsymbol{\sigma}_X^{\mathrm{T}}}\right] \tag{13}$$

where

$$\frac{\partial R_{\mathrm{FM}}}{\partial \beta_{\mathrm{FM}}} = \phi(\beta_{\mathrm{FM}}) \tag{14}$$

$$\frac{\partial \beta_{\mathrm{FM}}}{\partial \mu_g} = \frac{6\left(3\eta_g + 2\sigma_g^4\right) + 22\theta_g\mu_g}{\sqrt{36\sigma_g^2\left(3\eta_g + 2\sigma_g^4\right)^2 - 55{\theta_g}^2\left(5\eta_g + 7\sigma_g^4\right)}} \tag{15}$$

$$\frac{\partial\beta_{\mathrm{FM}}}{\partial\sigma_g} = \frac{\left(48\mu_g\sigma_g^3 + 22\theta_g\sigma_g\right)\left(36\sigma_g^2\left(3\eta_g + 2\sigma_g^4\right)^2 - 55\theta_g{}^2\left(5\eta_g + 7\sigma_g^4\right)\right)}{\left(\sqrt{36\sigma_g^2\left(3\eta_g + 2\sigma_g^4\right)^2 - 55\theta_g{}^2\left(5\eta_g + 7\sigma_g^4\right)}\right)^3} - \frac{\left[6\mu_g\left(3\eta_g + 2\sigma_g^4\right) + 11\theta_g\left(\mu_g^2 - \sigma_g^2\right)\right]\left(36\sigma_g\left(3\eta_g + 2\sigma_g^4\right)\left(3\eta_g + 6\sigma_g^4\right) - 770\theta_g^2\sigma_g^3\right)}{\left(\sqrt{36\sigma_g^2\left(3\eta_g + 2\sigma_g^4\right)^2 - 55\theta_g{}^2\left(5\eta_g + 7\sigma_g^4\right)}\right)^3} \tag{16}$$

$$\frac{\partial\beta_{\mathrm{FM}}}{\partial\theta_g} = \frac{11\left(\mu_g^2 - \sigma_g^2\right)\left[36\sigma_g^2\left(3\eta_g + 2\sigma_g^4\right)^2 - 55\theta_g{}^2\left(5\eta_g + 7\sigma_g^4\right)\right]}{\left(\sqrt{36\sigma_g^2\left(3\eta_g + 2\sigma_g^4\right)^2 - 55\theta_g{}^2\left(5\eta_g + 7\sigma_g^4\right)}\right)^3} + \frac{55\theta_g\left(5\eta_g + 7\sigma_g^4\right)\left[6\mu_g\left(3\eta_g + 2\sigma_g^4\right) + 11\theta_g\left(\mu_g^2 - \sigma_g^2\right)\right]}{\left(\sqrt{36\sigma_g^2\left(3\eta_g + 2\sigma_g^4\right)^2 - 55\theta_g{}^2\left(5\eta_g + 7\sigma_g^4\right)}\right)^3} \tag{17}$$

$$\frac{\partial\beta_{\mathrm{FM}}}{\partial\eta_g} = \frac{18\mu_g\left(36\sigma_g^2\left(3\eta_g + 2\sigma_g^4\right)^2 - 55\theta_g{}^2\left(5\eta_g + 7\sigma_g^4\right)\right)}{\left(\sqrt{36\sigma_g^2\left(3\eta_g + 2\sigma_g^4\right)^2 - 55\theta_g{}^2\left(5\eta_g + 7\sigma_g^4\right)}\right)^3} - \frac{\left[6\mu_g\left(3\eta_g + 2\sigma_g^4\right) + 11\theta_g\left(\mu_g^2 - \sigma_g^2\right)\right]\left[216\sigma_g^2\left(3\eta_g + 2\sigma_g^4\right) - 275\theta_g{}^2\right]}{2\left(\sqrt{36\sigma_g^2\left(3\eta_g + 2\sigma_g^4\right)^2 - 55\theta_g{}^2\left(5\eta_g + 7\sigma_g^4\right)}\right)^3} \tag{18}$$

$$\frac{\partial\mu_{g_z}}{\partial\boldsymbol{\mu}_X^{\mathrm{T}}} = \left[\frac{\partial g_z(\boldsymbol{X})}{\partial\mu_{X_1}}\frac{\partial g_z(\boldsymbol{X})}{\partial\mu_{X_2}}\cdots\frac{\partial g_z(\boldsymbol{X})}{\partial\mu_{X_n}}\right] \tag{19}$$

$$\begin{aligned}\frac{\partial\sigma_{g_z}^2}{\partial\boldsymbol{\mu}_X^{\mathrm{T}}} &= 2\left(\mathrm{C}_2(\boldsymbol{X})\frac{\partial g_z}{\partial\boldsymbol{\mu}_X}\right)^{\mathrm{T}}\frac{\partial^2 g_z}{\partial\boldsymbol{\mu}_X\partial\boldsymbol{\mu}_X^{\mathrm{T}}}\\ &= 2\frac{\partial g_z}{\partial\boldsymbol{\mu}_X^{\mathrm{T}}}\mathrm{C}_2(\boldsymbol{X})\frac{\partial^2 g_z}{\partial\boldsymbol{\mu}_X\partial\boldsymbol{\mu}_X^{\mathrm{T}}}\end{aligned} \tag{20}$$

$$\begin{aligned}\frac{\partial\sigma_{g_z}}{\partial\boldsymbol{\mu}_X^{\mathrm{T}}} &= \frac{1}{\sigma_{g_z}}\frac{\partial g_z}{\partial\boldsymbol{\mu}_X^{\mathrm{T}}}\mathrm{C}_2(\boldsymbol{X})\frac{\partial^2 g_z}{\partial\boldsymbol{\mu}_X\partial\boldsymbol{\mu}_X^{\mathrm{T}}}\\ \frac{\partial\theta_{g_z}}{\partial\boldsymbol{\mu}_X^{\mathrm{T}}} &= \frac{\partial g_z}{\partial\boldsymbol{\mu}_X^{\mathrm{T}}}\mathrm{C}_3(\boldsymbol{X})\frac{\partial}{\partial\boldsymbol{\mu}_X^{\mathrm{T}}}\left(\frac{\partial g_z}{\partial\boldsymbol{\mu}_X}\otimes\frac{\partial g_z}{\partial\boldsymbol{\mu}_X}\right)\\ &+ \frac{\partial g_z}{\partial\boldsymbol{\mu}_X^{\mathrm{T}}}\otimes\frac{\partial g_z}{\partial\boldsymbol{\mu}_X^{\mathrm{T}}}\mathrm{C}_3(\boldsymbol{X})^{\mathrm{T}}\frac{\partial}{\partial\boldsymbol{\mu}_X^{\mathrm{T}}}\left(\frac{\partial g_z}{\partial\boldsymbol{\mu}_X}\right)\end{aligned} \tag{21}$$

$$\frac{\partial\eta_{g_z}}{\partial\boldsymbol{\mu}_X^{\mathrm{T}}} = 2\left(\frac{\partial g_z}{\partial\boldsymbol{\mu}_X^{\mathrm{T}}}\otimes\frac{\partial g_z}{\partial\boldsymbol{\mu}_X^{\mathrm{T}}}\right)C_4(X)\frac{\partial}{\partial\boldsymbol{\mu}_X^{\mathrm{T}}}\left(\frac{\partial g_z}{\partial\boldsymbol{\mu}_X}\otimes\frac{\partial g_z}{\partial\boldsymbol{\mu}_X}\right) \tag{22}$$

If the first-order mean value of the Taylor series expansion of $g(\boldsymbol{X})$ is identified (i.e. $\mu_g = g(\boldsymbol{\mu}_X)$, where μ_g is a function of $\boldsymbol{\mu}_X$ and unrelated to $\boldsymbol{\sigma}_X$), then we have

$$\frac{\partial\mu_{g_z}}{\partial\boldsymbol{\sigma}_X^{\mathrm{T}}} = 0 \tag{23}$$

$$\begin{aligned}\frac{\partial\sigma_{g_z}}{\partial\boldsymbol{\sigma}_X^{\mathrm{T}}} &= \left(\frac{1}{2\sigma_{g_z}}\right)\frac{\partial\sigma_{g_z}^2}{\partial\boldsymbol{\sigma}_X^{\mathrm{T}}}\\ &= \left(\frac{1}{\sigma_{g_z}}\right)\boldsymbol{\sigma}_X^{\mathrm{T}}\mathrm{diag}\left(\frac{\partial g_z}{\partial\boldsymbol{\mu}_X}\right)[\boldsymbol{\rho}]\mathrm{diag}\left(\frac{\partial g_z}{\partial\boldsymbol{\mu}_X}\right)\end{aligned} \tag{24}$$

$$\frac{\partial\theta_{g_z}}{\partial\boldsymbol{\sigma}_X^{\mathrm{T}}} = \boldsymbol{\sigma}_X^{\mathrm{T}}\boldsymbol{C}_{\mu3}(\boldsymbol{X})\frac{\partial}{\partial\boldsymbol{\sigma}_X^{\mathrm{T}}}(\boldsymbol{\sigma}_X\otimes\boldsymbol{\sigma}_X) + (\boldsymbol{\sigma}_X\otimes\boldsymbol{\sigma}_X)^{\mathrm{T}}\boldsymbol{C}_{\mu3}(\boldsymbol{X})^{\mathrm{T}} \tag{25}$$

$$\frac{\partial\eta_{g_z}}{\partial\boldsymbol{\sigma}_X^{\mathrm{T}}} = 2\left(\boldsymbol{\sigma}_X^{\mathrm{T}}\otimes\boldsymbol{\sigma}_X^{\mathrm{T}}\right)\boldsymbol{C}_{\mu4}(X)\frac{\partial}{\partial\boldsymbol{\sigma}_X^{\mathrm{T}}}(\boldsymbol{\sigma}_X\otimes\boldsymbol{\sigma}_X) \tag{26}$$

where $\varphi(\cdot)$ represents a standard normal probability density function. The known condition and the results of the calculation of relevant data and reliability are combined and substituted into the equations for the reliability sensitivity of a structural component (equations (12) and (13)). Thus, information that relates to the reliability sensitivity (i.e. $\partial R_{\mathrm{FM}}/\partial\boldsymbol{\mu}_X$ and $\partial R_{\mathrm{FM}}/\partial\boldsymbol{\sigma}_X$) can be obtained.

Reliability sensitivity is used to evaluate the level of impact of a certain factor on the reliability of a structural component. To uniformly describe the level of impact of various factors on the reliability of a structural component, the reliability variation gradient at the nominal point is generally selected as the sensitivity factor. Therefore, the reliability sensitivity gradient can be expressed as follows

$$\mathrm{Grad}\frac{\mathrm{D}R_{\mathrm{FM}}\left(\mu_{X_i},\sigma_{X_i}\right)}{\mathrm{D}\boldsymbol{X}} = \sqrt{\left(\frac{\partial R_{\mathrm{FM}}}{\partial\mu_{X_i}}\right)^2 + \left(\frac{\partial R_{\mathrm{FM}}}{\partial\sigma_{X_i}}\right)^2} \tag{27}$$

Reliability-based robust design

Structural reliability-based robust optimal design can be expressed using the following mathematical model

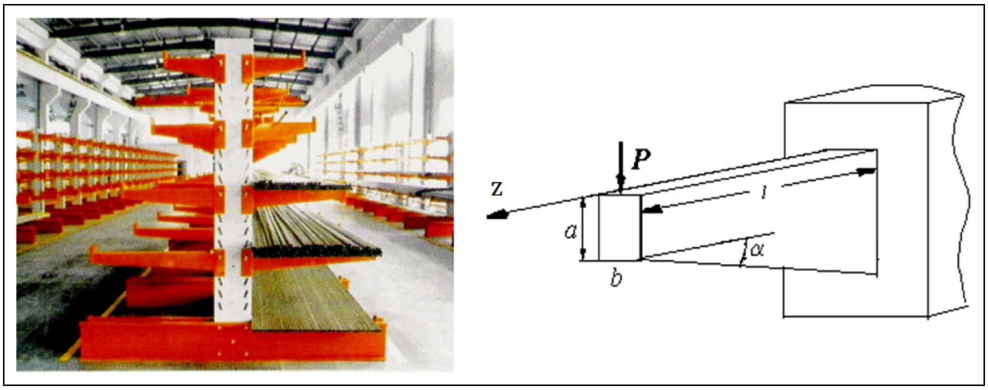

Figure 3. Actual structural and mechanical model of a cantilever bracket.

$$\left.\begin{array}{lll} \min & f(\boldsymbol{X}) = \sum_{k=1}^{n} w_k f_k(\boldsymbol{X}) & \\ \text{s.t.} & g_z - \Phi^{-1}(R_0)\sigma_{g_z} \geq 0 & \\ & g_i(\boldsymbol{X}) \geq 0 & (i = 1, 2, \ldots, l) \\ & h_j(\boldsymbol{X}) = 0 & (j = 1, 2, \ldots, s) \end{array}\right\} \tag{28}$$

where R_0 represents the reliability specified in the design requirements; $\boldsymbol{X}$ represents the basic random vectors, including the design variable vectors (denoted by $\boldsymbol{x} = (x_1 x_2 \cdots\ x_m)^{\mathrm{T}}$) and random parameter vectors; and w_k represents the weighting factor of the sub-objective function $f_k(\boldsymbol{X})$ ($w_k \geq 0$). The value of w_k is determined by the order of magnitude and degree of importance of each sub-objective function. In this study, w_k is determined using the weighting combination method, that is

$$\left.\begin{array}{l} w_1 = \dfrac{f_k\left(\boldsymbol{X}^{*1}\right) - f_k\left(\boldsymbol{X}^{*k}\right)}{\left[f_1\left(\boldsymbol{X}^{*k}\right) - f_1\left(\boldsymbol{X}^{*1}\right)\right] + \left[f_2\left(\boldsymbol{X}^{*(k-1)}\right) - f_2\left(\boldsymbol{X}^{*2}\right)\right] + \cdots + \left[f_k\left(\boldsymbol{X}^{*1}\right) - f_k\left(\boldsymbol{X}^{*k}\right)\right]} \\ w_2 = \dfrac{f_{k-1}\left(\boldsymbol{X}^{*2}\right) - f_{k-1}\left(\boldsymbol{X}^{*(k-1)}\right)}{\left[f_1\left(\boldsymbol{X}^{*k}\right) - f_1\left(\boldsymbol{X}^{*1}\right)\right] + \left[f_2\left(\boldsymbol{X}^{*(k-1)}\right) - f_2\left(\boldsymbol{X}^{*2}\right)\right] + \cdots + \left[f_k\left(\boldsymbol{X}^{*1}\right) - f_k\left(\boldsymbol{X}^{*k}\right)\right]} \\ \vdots \\ w_k = \dfrac{f_1\left(\boldsymbol{X}^{*k}\right) - f_1\left(\boldsymbol{X}^{*1}\right)}{\left[f_1\left(\boldsymbol{X}^{*k}\right) - f_1\left(\boldsymbol{X}^{*1}\right)\right] + \left[f_2\left(\boldsymbol{X}^{*(k-1)}\right) - f_2\left(\boldsymbol{X}^{*2}\right)\right] + \cdots + \left[f_k\left(\boldsymbol{X}^{*1}\right) - f_k\left(\boldsymbol{X}^{*k}\right)\right]} \end{array}\right\} \tag{29}$$

Numerical example

Figure 3 shows a tapered beam under a vertical pressure. Each geometric cross-sectional parameter can be considered to independently follow a normal distribution. The mean and variance of the tapered beam parameters are as follows: cross-sectional thickness b = (12, 0.06) mm; free-end height a = (18, 0.09) mm; slope of the tapered beam α = arctan(0.12, 0.006); and length of the tapered beam l = (500, 2.5) mm. The probability distributions of the load and the strength parameter are unknown; however, the first four moments of the load and the strength parameter are known. The first four moments of the load borne by the beam P = 3400 N, 170 N, $7.3756 \times 10^5\,\mathrm{N}^3$, $2.539 \times 10^9\ \mathrm{N}^4$ and the first four moments of the tensile strength of the material r = 221 MPa, 11.05 MPa, $2.0255 \times 10^2\,\mathrm{MPa}^3$, $4.532 \times 10^4\,\mathrm{MPa}^4$. Here, a reliability sensitivity analysis is performed on this structural component, and a reliability-based robust design is developed for this structural component.

Reliability analysis of the tapered beam

Structural brackets and various types of bases are often involved in structural design. These structures are generally composed of shaped steel bars, plates, and some prefabricated structural components to satisfy the mechanical strength, stiffness, and appearance requirements. The bending stress of a tapered beam at any arbitrary cross section z is

$$S_z(\boldsymbol{X}) = \frac{6P(l-z)}{b[a + \tan\alpha(l-z)]^2} \tag{30}$$

Transversal force-caused bending is common in engineering structures. As the ratio of beam span and cross-sectional height is $n \geq 5$, the shear stress resulting from the load is not considered. According to the stress–strength interference theory, the state equation expressed with the ultimate stress state is expressed as follows

$$g_z(\boldsymbol{X}) = r - \frac{6P(l-z)}{b[a + \tan\alpha(l-z)]^2} \tag{31}$$

where r represents the material strength of the tapered beam; $\boldsymbol{X} = [a\ b\ r\ P\ l\ \tan\alpha]^{\mathrm{T}}$ represents the basic random variable vectors, and z represents the coordinates of any arbitrary cross section of the tapered beam. All probabilistic numerical characteristics of $\boldsymbol{X}$ are known. However, the probability distributions of some random variables are unknown.

Table 1. Reliability sensitivity to μ_X and σ_X before optimization.

Random variables	$\partial R/\partial \boldsymbol{\mu}_X$	$\partial R/\partial \boldsymbol{\sigma}_X$	Gradient of sensitivity
a	1.049694×10^2	-7.03445	1.905708×10^2
b	1.572851×10^2	-10.9063	1.5766×10^2
p	-0.5352×10^{-3}	-0.3949×10^{-2}	6.6513×10^{-4}
l	0.1321×10^{-1}	-7.3199×10^{-4}	1.3234×10^{-2}
$\tan\alpha$	16.2693	-11.2668	1.9790×10
r	0.89003×10^{-8}	-7.2570×10^{-9}	1.1484×10^{-8}

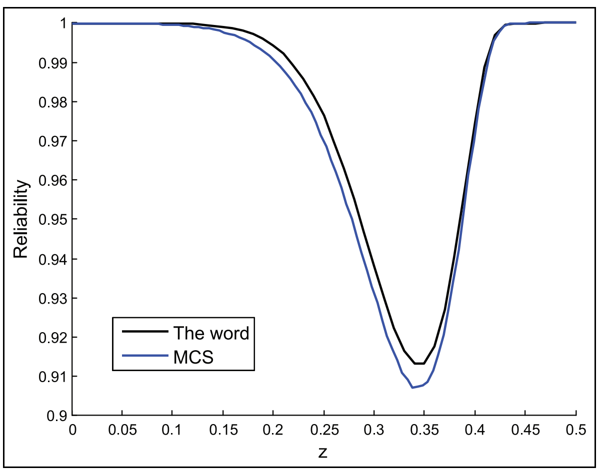

Figure 4. Reliability curves of the tapered beam.

Volume (V) is one of the important reference values for the reliability-based design of a tapered beam and is a main target for a lightweight design. The selected tapered beam has a V of

$$V = abl + \frac{bl^2 \tan\alpha}{2} \tag{32}$$

The first four moments of the state function of the VCS structural component are determined by substituting the known condition and relevant data into the expressions of the first four moments of the state function of a VCS structural component (equations (4)–(7)). Then, a reliability analysis and calculation are performed by substituting the known condition and relevant data into the equations for β_{FM} (equation (10)) and R_{FM} (equation (11)). By substituting the known condition, β_{FM} and R_{FM} curves with respect to z are obtained by calculation, as shown in Figure 4.

As demonstrated in Figure 4, the β_{FM} and R_{FM} curves of the tapered beam exhibit a parabolic shape. The β_{FM} and R_{FM} of the tapered beam vary with z. The minimum β_{FM} and R_{FM} occur near 0.345 m, that is, the cross section at $z = 345\,\mathrm{mm}$ is a dangerous cross section. Thus, when developing a reliability-based design for a VCS structural component, balanced reliability should be effectively ensured based on the reliability analysis results.

Based on the equations for the β_{FM} (equation (10)), R_{FM} (equation (11)), and V (equation (32)) of a VCS structural component, the V, β_{FM}, and R_{FM} of the tapered beam at the dangerous cross section are

$V_0 = 288\,\mathrm{mm}^3$

$\beta_{\mathrm{FM}} = 1.36064$

$R_{\mathrm{FM}} = 0.91319$

The reliability of the VCS structural component is also calculated by simulation using the Monte Carlo method, and the result, which is denoted by R_{MC}, is

$R_{\mathrm{MC}} = 0.90605$

where R_{MC} represents the reliability obtained from the numerical simulation based on 10^5 samples using the Monte Carlo method. The calculation results demonstrate that the results obtained using the proposed method are consistent with the results obtained from the numerical simulation using the Monte Carlo method.[38–43]

Reliability sensitivity analysis of the tapered beam

A reliability sensitivity analysis of the tapered beam is performed via calculation by substituting the known condition and relevant data into the expressions of the sensitivity of R_{FM} of a structural component (equations (12) and (13)). The data in Table 1 list the values of the reliability sensitivity of the structural component with non-normally distributed parameters to $\boldsymbol{\mu}_X$ and $\boldsymbol{\sigma}_X$, as well as the R_{FM} sensitivity gradient.

The reliability sensitivity analysis demonstrates that the reliability sensitivity of the entire tapered beam to each $\boldsymbol{X}$ reaches the extreme value at the dangerous location. The dangerous cross section is the most sensitive to variations in $\boldsymbol{X}$. A comparison with the R_{FM} curve shown in Figure 4 indicates that the location on the tapered beam with high reliability is the least sensitive to variations in $\boldsymbol{X}$. As demonstrated in Table 1, the reliability sensitivity of the tapered beam to each r, b, a, l, and $\tan\alpha$ has a positive value. These random variables each have a positive impact on the R_{FM} of the tapered beam, that is, an increase in the mean value of each r, b, a, l, and $\tan\alpha$ will cause an increase in the

R_{FM} of the structural component—the R_{FM} of the tapered beam increases as each r, b, a, l, and $\tan\alpha$ increases. Conversely, the sensitivity of the R_{FM} of the tapered beam to P (i.e. force applied at the free end of the tapered beam) has a negative value. P has a negative impact on the R_{FM} of the tapered beam, that is, the R_{FM} of the tapered beam decreases as P increases and the reliability sensitivity of the tapered beam to P reaches the extreme value at the dangerous location. A change in b will have the most significant impact on the R_{FM} of the tapered beam, followed by a, $\tan\alpha$, l, P, and r. In addition, Table 1 also demonstrates that the reliability sensitivity of the tapered beam to the variance of each random variable has a negative value. The R_{FM} of the tapered beam decreases as the variance of each basic random variable increases, that is, the variance of each basic random variable has a negative impact on the R_{FM} of the tapered beam.

Reliability-based robust design for the tapered beam

A reliability-based robust optimal design that satisfies the design reliability requirement ($R_0 = 0.99$) and minimizes the weight of the tapered VCS beam is developed.

Determining design variables. By analyzing the main parameters that affect the reliability of the tapered beam, three parameters, namely, a, b, and $\tan\alpha$, are selected as the design variables when developing a reliability-based robust optimal design model. Thus, the design variable vectors are $x = [a\ b\ \tan\alpha]^{\mathrm{T}}$.

Establishing objective functions. The weight of the tapered beam can be minimized by minimizing its V. Therefore, the first optimization objective of the reliability-based robust optimal design is

$$f_1(\boldsymbol{X}) = V \tag{33}$$

To eliminate the reliability sensitivity of the tapered beam to the design parameters (i.e. to enable the tapered beam to be robust), the sensitivity function of the reliability constraint to the design parameters is selected as the second optimization objective of the reliability-based robust optimal design, that is

$$f_2(\boldsymbol{X}) = \sqrt{\left[\frac{\partial R_{\mathrm{FM}}}{\partial a}\right]^2 + \left[\frac{\partial R_{\mathrm{FM}}}{\partial b}\right]^2 + \left[\frac{\partial R_{\mathrm{FM}}}{\partial \tan\alpha}\right]^2} \tag{34}$$

Establishing constraint conditions. The tapered beam needs to satisfy certain reliability requirements. Thus, we have the following reliability constraint condition

$$R_{\mathrm{FM}} - R_0 \geq 0 \tag{35}$$

The geometric dimensions of the tapered beam also need to satisfy certain design conditions. Thus, we have the following inequality constraint conditions

$$10 \leq a \leq 20$$

$$8 \leq b \leq 15$$

$$0.1 \leq \tan\alpha \leq 0.15$$

Reliability-based robust optimal design. The design values of the parameters are selected as the initial values for optimization: $x = [a\quad b\quad \tan\alpha] = [0.019822,\ 0.010452,\ 0.14787]$. The parameters obtained from reliability-based robust optimization are as follows

$V = 293.36\,\mathrm{mm}^3$
$a = 19.822\,\mathrm{mm}$
$b = 10.452\,\mathrm{mm}$
$\tan\alpha = 0.1479$

The β_{FM} and R_{FM} of the tapered beam after optimization are

$\beta_{\mathrm{FM}} = 3.4010$
$R_{\mathrm{FM}} = 0.99966$

The calculation results are as follows. (1) $R_{\mathrm{FM}} = 0.99966$ satisfies the reliability-based robust optimal design requirement for the reliability of the tapered beam, that is, $R_0 = 0.99$. (2) R_0 is considerably higher than the initial reliability ($R_{\mathrm{FM}} = 0.91319$), and the V of the tapered beam is correspondingly increased by $\Delta V = V - V_0 = 293.36\,\mathrm{mm}^3 - 288\,\mathrm{mm}^3 = 5.36\,\mathrm{mm}^3$. This finding demonstrates that the reliability-based robust design reaches the VCS structural component design goal—balanced reliability—and that the reliability theory and technique are effective and practical lightweight techniques.

Figure 5 shows the variation curve of the R_{FM} of the tapered beam with z after optimization. Compared to

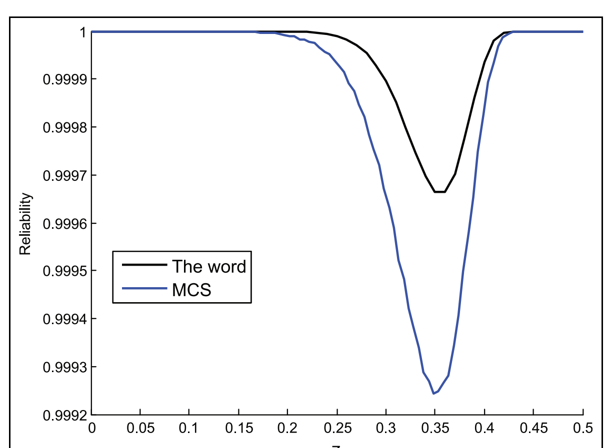

Figure 5. β_{FM} and R_{FM} curves after optimization.

Table 2. Reliability sensitivity to μ_X and σ_X after optimization.

Random variables	$\partial R/\partial \boldsymbol{\mu}_X$	$\partial R/\partial \boldsymbol{\sigma}_X$	Gradient of sensitivity
a	0.7115	-9.2846×10^{-2}	0.7175
b	1.3962	-0.2047	1.4111
p	-0.3940×10^{-4}	-0.6984×10^{-4}	8.0188×10^{-6}
l	3.1559×10^{-3}	-2.3458×10^{-4}	3.1646×10^{-3}
tanα	0.11022	-0.1664	1.9962×10^{-1}
r	0.7335×10^{-10}	-0.1477×10^{-9}	1.6456×10^{-10}

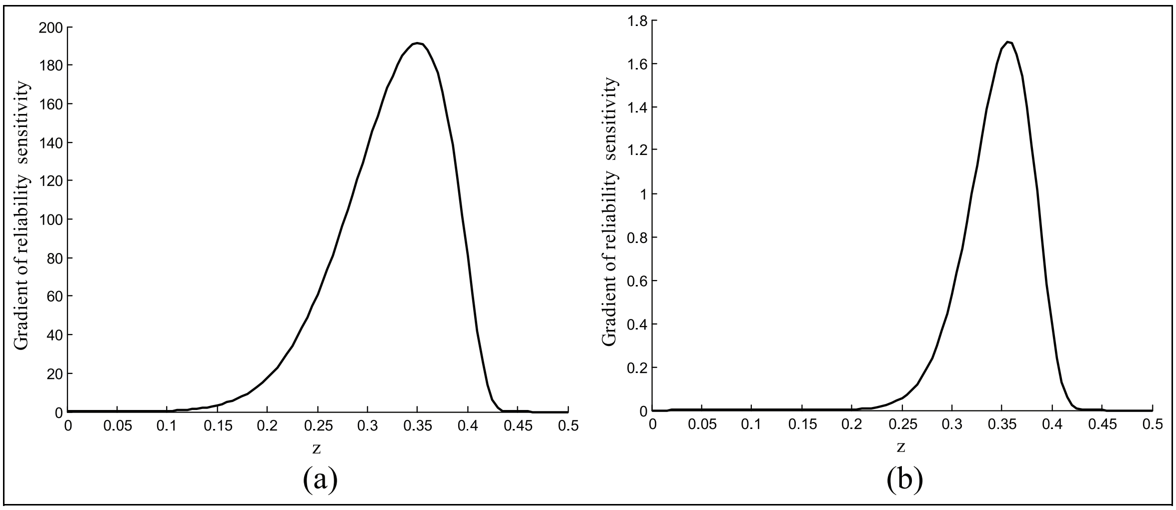

Figure 6. Variation curves of the R_{FM} sensitivity gradient with z: (a) variation curve of the R_{FM} sensitivity gradient before optimization and (b) variation curve of the R_{FM} sensitivity gradient after optimization.

the R_{FM} shown in Figure 4, the R_{FM} of the tapered beam is significantly higher after optimization.

A comparison of R_{FM} before and after the reliability-based robust optimal design indicates that the numerical value of R_{FM} significantly increases, and the range within which R_{FM} varies also significantly decreases after optimization, which demonstrates that the reliability-based robust optimal design method is effective and can produce a balanced result. Therefore, research on the reliability of a VCS structural component can ensure the reliability level, reflect the actual condition of the VCS structural component, and ensure that the design working performance of the VCS structural component is more consistent with its actual working performance. Research on the reliability of a VCS structural component can facilitate the development of a lightweight design, ensure that the working performance and parameters of the VCS structural component are optimal, and help reach design goals, such as weight reduction, efficiency enhancement, energy saving, environmental protection, performance enhancement, and a safe and reliable design.

The values of $x = [a \ b \ \tan\alpha]^{\mathrm{T}}$ after the reliability-based robust design ($a = 19.822\,\mathrm{mm}$, $b = 10.452\,\mathrm{mm}$, and $\tan\alpha = 0.1479$) are selected for a reliability sensitivity analysis. Table 2 lists the values of the reliability sensitivity of the VCS structural component to $\boldsymbol{\mu}_X$ and $\boldsymbol{\sigma}_X$ and the corresponding R_{FM} sensitivity gradients after optimization.

The reliability sensitivity analysis results obtained before and after the reliability-based robust optimal design indicate that the numerical value of the reliability sensitivity significantly decreases after the reliability-based robust optimal design, which ensures stable reliability and eliminates the reliability sensitivity of the VCS structural component to the design parameters for interference factors, enhances the safety, reliability, and robustness of the VCS structural component, and attains the reliability-based robust design goals and effect.

The reliability sensitivity of the tapered beam at any arbitrary location can be calculated using equations (12) and (13). The R_{FM} sensitivity gradient of the tapered beam at any arbitrary location can be calculated using the expression of the R_{FM} sensitivity gradient of a structural component (equation (27)). Figure 6 shows the variation curves of the R_{FM} sensitivity gradient of the VCS structural component with z plotted based on the variation patterns of the mean value and mean square error of the reliability sensitivity of the VCS structural component with z.

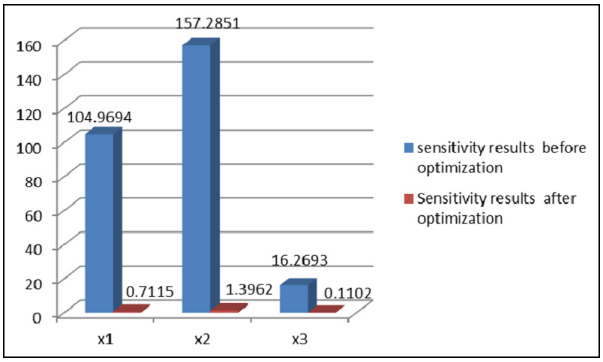

Figure 7. Reliability sensitivity to the mean value of *x*.

The previously mentioned calculation results demonstrate the following conclusions. (1) The higher the R_{FM} of the VCS structural component $R_{FM} = \Phi(\beta_{FM})$, the gentler the variation curve of R_{FM} with z, and the smaller the numerical value of the R_{FM} sensitivity gradient, that is, the lower the sensitivity of R_{FM} of the VCS structural component to variations in the design parameters (the more robust the VCS structural component). (2) The numerical value of the R_{FM} sensitivity gradient significantly decreases after the reliability-based robust optimal design. This finding demonstrates that the reliability-based robust optimal design yields notable results, and the reliability-based robust optimal design method is effective and practical.

Figure 7 shows the comparison of the reliability sensitivity to the mean values of $\boldsymbol{x}$ before and after the reliability-based robust optimal design. Figure 7 demonstrates the level of impact of variations in each random variable on the reliability sensitivity of the VCS structural component and provides the reliability sensitivity to the mean value of $\boldsymbol{x}$.

Figure 7 demonstrates the following results. (1) The R_{FM} of the VCS structural component varies with the design parameters. A change in b will have the most significant impact on the R_{FM} of the VCS structural component, followed by a and α. Therefore, variations in the sensitive parameters should be strictly controlled when designing the shape and dimensions of the VCS structural component. (2) The numerical values of the reliability sensitivity to $\boldsymbol{x}$ are smaller after the reliability-based robust optimal design. This finding demonstrates that the R_{FM} of the VCS structural component is less sensitive to variations in the design variables (i.e. the VCS structural component is more robust) after the optimization, and the reliability-based robust optimal design goal is achieved.

Conclusion

In structural design, the reliability-based robust optimal design method can be employed to ensure that the reliability of the design structure is stable when the design parameters undergo variations (i.e. eliminated reliability sensitivity of the structure to the design parameters). By doing so, the objectives of satisfying the reliability requirements and reducing cost can be achieved. In this article, the reliability-based design method is combined with the robust design theory, the function of reliability sensitivity is included in the objective function of the reliability-based optimal design model, and reliability-based robust optimal design is converted to a multi-objective optimization problem that satisfies the reliability requirements. Based on this idea, mathematical models for reliability sensitivity analysis and reliability-based robust optimal design of VCS structural components are established. Reliability sensitivity analysis and reliability-based robust optimal design theories and methods for VCS structural components are proposed. A case study is conducted to illustrate the proposed method. In the case study, an in-depth reliability sensitivity analysis is performed on a VCS tapered beam, and a reliability-based robust design is also developed for this tapered beam. Ideal analysis and design results are obtained, which forms a solid foundation for the reliability sensitivity analysis and reliability-based robust design of VCS structural components in practical engineering applications.

Declaration of conflicting interests

The author(s) declared no potential conflicts of interest with respect to the research, authorship, and/or publication of this article.

Funding

The author(s) received no financial support for the research, authorship, and/or publication of this article.

References

1. Ang AHS and Tang WH. *Probability concepts in engineering planning and design: basic principles, vol.1*. New York: Wiley, 1975.
2. Kapur KC and Lamberson LR. *Reliability in engineering design*. New York: John Wiley & Sons, 1977.
3. Dhillon BS and Singh C. *Engineering reliability*. New York: John Wiley & Sons, 1981.
4. Henley EJ and Kumamoto H. *Reliability engineering and risk assessment*. Englewood Cliffs: Prentice-Hall, Inc., 1981.
5. Billinton B and Allan RN. *Reliability evaluation of engineering systems*. London: Pitman Books Limited, 1983.
6. O'Connor PDT. *Practical reliability engineering*. New York: John Wiley & Sons, 1984.
7. Frangopol DM. *Life-cycle performance of deteriorating structures: assessment, design, and management*. Reston, VA: ASCE Publications, 2004.

8. Ellingwood B and Kanda J. *Structural safety and its quality assurance*. Reston, VA: *ASCE Publications*, 2005.
9. Madsen HO, Krenk S and Lind NC. *Methods of structural safety*. New York: Dover Publications, 2006.
10. Nowak AS and Collins KR. *Reliability of structures*. Florida: CRC Press, 2012.
11. Gaspar B and Soares CG. Hull girder reliability using a Monte Carlo based simulation method. *Probabilist Eng Mech* 2013; 31: 65–75.
12. Melchers RE and Ahammed M. A fast approximate method for parameter sensitivity estimation in Monte Carlo structural reliability. *Comput Struct* 2004; 82: 55–61.
13. Sues RH and Cesare MA. System reliability and sensitivity factors via the MPPSS method. *Probabilist Eng Mech* 2005; 20: 148–157.
14. Zhang YM, He XD, Liu QL, et al. Reliability sensitivity of automobile components with arbitrary distribution parameters. *Proc IMechE Part D: J Automobile Engineering* 2005; 219: 165–182.
15. Wu YT and Mohanty S. Variable screening and ranking using sampling-based sensitivity measures. *Reliab Eng Syst Safe* 2006; 91: 634–647.
16. Zhang YM, He XD, Liu QL, et al. Reliability-based optimization and robust design of coil tube-spring with non-normal distribution parameters. *Proc IMechE Part C: J Mechanical Engineering Science* 2005; 219: 567–576.
17. Zhang YM, He XD, Liu QL, et al. An approach of robust reliability design for mechanical components. *Proc IMechE Part E: J Process Mechanical Engineering* 2005; 219: 275–283.
18. Zhang YM, He XD, Liu QL, et al. Robust reliability design of banjo flange with arbitrary distribution parameters. *J Press Vess: T ASME* 2005; 127: 408–413.
19. Zhang YM, He XD, Liu QL, et al. Robust reliability design of vehicle components with arbitrary distribution parameters. *Int J Automot Techn* 2006; 7: 859–866.
20. Motta RD and Afonso SMB. An efficient procedure for structural reliability-based robust design optimization. *Struct Multidiscip O* 2016; 54: 511–530.
21. Salazar DE and Rocco CM. Solving advanced multi-objective robust designs by means of multiple objective evolutionary algorithms (MOEA): A reliability application. *Reliab Eng Syst Safe* 2007; 92: 697–706.
22. Youn BD and Xi ZM. Reliability-based robust design optimization using the eigenvector dimension reduction (EDR) method. *Struct Multidiscip Optim* 2009; 37: 475–492.
23. Lagaros ND, Plevris V and Papadrakakis M. Neurocomputing strategies for solving reliability-robust design optimization problems. *Eng Computation* 2010; 27: 819–840.
24. Yadav OP, Bhamare SS and Rathore A. Reliability-based robust design optimization: a multi-objective framework using hybrid quality loss function. *Qual Reliab Eng Int* 2010; 26: 27–41.
25. Wang Z, Huang HZ and Liu Y. A unified framework for integrated optimization under uncertainty. *J Mech Des: T ASME* 2010; 132: 0510081–0510088.
26. Wang Z, Huang HZ and Du X. Optimal design accounting for reliability, maintenance, and warranty. *J Mech Des: T ASME* 2010; 132: 0110071–0110078.
27. Martowicz A and Uhl T. Reliability- and performance-based robust design optimization of MEMS structures considering technological uncertainties. *Mech Syst Signal Pr* 2012; 32: 44–58.
28. Yu H, Gillot F and Ichchou M. Reliability based robust design optimization for tuned mass damper in passive vibration control of deterministic/uncertain structures. *J Sound Vib* 2013; 332: 2222–2238.
29. Paiva RM, Crawford C and Suleman A. Robust and reliability-based design optimization framework for wing design. *AIAA J* 2014; 52: 711–724.
30. Wang PF, Wang ZQ and Almaktoom AT. Dynamic reliability-based robust design optimization with time-variant probabilistic constraints. *Eng Optimiz* 2014; 46: 784–809.
31. Qui J, Zhang J, Ma Y, et al. Reliability-based robust design for kinematic accuracy of a mechanism with axiomatic theory. *Proc IMechE Part G: J Aerospace Engineering*. Epub ahead of print 14 June 2017. DOI: 10.1177/0954410017714005.
32. Boiangiu M, Ceausu V and Untaroiu CD. A transfer matrix method for free vibration analysis of Euler-Bernoulli beams with variable cross section. *J Vib Control* 2016; 22: 2591–2602.
33. Kang HS, Joo BD, Li M, et al. Enhancing hydroformability of nonaxisymmetric part with variable cross section. *Adv Mech Eng* 2015; 7: 1–7.
34. Li J, Zhou L, Hua X, et al. Transmission loss of variable cross section apertures. *J Vib Acoust* 2014; 136: 044501.
35. Jun L, Xiangsheng X and Qiang C. An investigation of the variable cross-section extrusion process. *Int J Adv Manuf Tech* 2017; 91: 453–461.
36. Zhang TX. Matrix description of differential relations of moment functions in structural reliability sensitivity analysis. *Appl Math Mech-Engl* 2017; 38: 57–72.
37. Zhang TX and He D. An improved high-order statistical moment method for structural reliability analysis with insufficient data. *Proc IMechE Part C: J Mechanical Engineering Science*. Epub ahead of print 27 February 2017. DOI: 10.1177/0954406217694662.
38. Zio E. *The Monte Carlo simulation method for system reliability and risk analysis*. London: Springer, 2013.
39. Zhu SP, Foletti S and Beretta S. Probabilistic framework for multiaxial LCF assessment under material variability. *Int J Fatigue* 2017; 103: 371–385
40. Zhu Sp, Huang HZ, Peng W, et al. Probabilistic physics of failure-based framework for fatigue life prediction of aircraft gas turbine discs under uncertainty. *Reliab Eng Syst Safe* 2016; 146: 1–12.
41. Meng D, Li YF, Huang HZ, et al. Reliability-based multidisciplinary design optimization using subset simulation analysis and its application in the hydraulic transmission mechanism design. *J Mech Design* 2015; 137: 051402.
42. Meng D, Zhang H and Huang T. A concurrent reliability optimization procedure in the earlier design phases of complex engineering systems under epistemic uncertainties. *Adv Mech Eng* 2016; 8: 1–8.
43. Meng D, Huang HZ, Wang Z, et al. Mean-value first-order saddlepoint approximation based collaborative optimization for multidisciplinary problems under aleatory uncertainty. *J Mech Sci Technol* 2014; 28: 3925–3935.